Modeling the effects of acid amplifiers on photoresist stochastics

Gregg M. Gallatin[a], Patrick P. Naulleau[b], and Robert Brainard[c]
a Center for Nanoscale Science and Technology,
National Institute of Standards and Technology, Gaithersburg, MD 20899
b Center for X-Ray Optics, Lawrence Berkeley National Laboratory, Berkeley, CA 94720
c College of Nanoscale Science and Engineering, Albany, NY 12203

February 22, 2012

ABSTRACT

The tradeoff between Resolution, Line Edge Roughness (LER) and Sensitivity, the so called RLS tradeoff, continues to be a difficult challenge, especially for EUV lithography. Acid amplifiers have recently been proposed as a method to improve upon the overall RLS performance of EUV resists. Here we discuss a simulation approach to study the issue. The model extends the standard reaction diffusion equation to explicitly capture the stochastic behavior of exposure, photo-acid generation and acid amplification. Using this model the impact acid amplifiers have on the RLS tradeoff is studied under a variety of resist conditions.

1 Introduction

Extreme ultraviolet (EUV) lithography continues to be a strong candidate for a commercially viable solution to next generation lithography. However, further development of chemically amplified photoresists for use with EUV is critical to meet the future photolithographic requirements of the microelectronics industry. EUV resists must simultaneously meet three requirements: high resolution (below 22 nm), low line edge roughness (LER)[1] and high sensitivity.[2] It has been proposed that the best way to simultaneously improve these three properties is to increase the number of strong acids generated per photon absorbed during exposure[3] and that acid amplifiers potentially could achieve this goal. Acid amplifiers (AAs) are compounds that decompose in the presence of other acid molecules to generate more acid molecules via acid-catalyzed mechanisms.[4] When the product acid is strong enough to catalyze the decomposition of the AA, the decomposition occurs autocatalytically.[5] Based on this definition, the chemical structure of AA molecules should contain an acid sensitive functional group and an acid precursor.

Synthetic efforts in this direction have focussed on designing thermally stable AAs that produce fluorinated sulfonic acids for use in phenolic EUV resists.[6] In that work the chemical structure of the AAs was varied to give a range of reactivities. These AAs consisted of three parts, a body, an acid-sensitive trigger (either hydroxyl, methoxy, acetate or ketal), and a sulfonic acid precursor. There are two decomposition mechanisms that can occur to produce an acid. The undesirable decomposition pathway is uncatalyzed thermal decomposition which results in the formation of an olefin byproduct and an acid. The desired acid generation pathway is via acid catalyzed decomposition. During autocatalysis, the trigger undergoes acidolysis yielding an allylic sulfonic ester. This olefin intermediate allows the sulfonic ester to thermally decompose via an E1 or E2 elimination reaction

more rapidly than the starting AA, yielding a second double bond alkene fragment and a sulfonic acid.

Several acid amplifiers have been reported in the literature. The reactivity of these compounds is highly dependent upon the structure of the body, trigger and acid precursor.[7] Triggers that have been studied are alcohols[8,9,10] ketals,[11] carbonates[12] and tert-alkylcarboxy groups.[13] The acid generated by these compounds is almost always a sulfonic acid, and typically toluene sulfonic acid. Only two acid amplifiers previously reported in the literature produce fluorinated sulfonic acids.[14] With the exception of Kruger, et. al.,[6] the AAs presented in the literature do not meet the requirements for use in EUV photoresists.

There are many contributors to line edge roughness (LER) in resist features on a wafer. The most widely studied contributors are the stochastic effects of exposure, deprotection and development of the resist itself.[15,16,17,18] Mask roughness also contributes.[19]

Here we present a model which includes the effects of exposure, photoacid generator (PAG), base and acid amplifier statistics. The model is based on an extension of the standard reacton-diffusion equations, which account for acid-base neutralization, to include acid amplification as well. The term added to the acid rate equation to account for acid amplification is of exactly the same form as that already present to represent acid-base neutralization. Of course this added term is positive rather than negative which causes amplification rather than neutralization. An additional equation is also required to account for depletion of the AA.

The paper is organized as follows. Section 2 discusses the equations and the approach used to obtain a numerical solution. Section 3 presents some illustrative results of the model. Section 4, the conclusion, discussed these results in relation to experimental data.[6]

2   Modeling Acid Amplification with Stochastics

To include acid amplification we modify the standard equations for modeling exposure and the post exposure bake(PEB)[20,21,22] to be

$$\rho_A\left(\vec{r},0\right) = \rho_{PAG}\left(1 - \exp\left[-\alpha q E\left(\vec{r}\right)\right]\right) \tag{1}$$

$$\frac{\partial \rho_D\left(\vec{r},t\right)}{\partial t} = -k_D\rho_A\left(\vec{r},t\right)\left(1 - \rho_D\left(\vec{r},t\right)\right) \tag{2}$$

$$\frac{\partial \rho_A\left(\vec{r},t\right)}{\partial t} = D_A\vec{\nabla}^2\rho_A\left(\vec{r},t\right) + \left(k_{AA}\rho_{AA}\left(\vec{r},t\right) - k_{AB}\rho_B\left(\vec{r},t\right)\right)\rho_A\left(\vec{r},t\right) \tag{3}$$

$$\frac{\partial \rho_B\left(\vec{r},t\right)}{\partial t} = D_B\vec{\nabla}^2\rho_B\left(\vec{r},t\right) - k_{AB}\rho_B\left(\vec{r},t\right)\rho_A\left(\vec{r},t\right) \tag{4}$$

$$\frac{\partial \rho_{AA}\left(\vec{r},t\right)}{\partial t} = D_{AA}\vec{\nabla}^2\rho_{AA}\left(\vec{r},t\right) - k_{AA}\rho_{AA}\left(\vec{r},t\right)\rho_A\left(\vec{r},t\right) \tag{5}$$

Here $\rho_A\left(\vec{r},t\right), \rho_B\left(\vec{r},t\right)$,and $\rho_{AA}\left(\vec{r},t\right)$ are the number of acid, base and AA molecules/volume at $\vec{r}$ at time t, respectively, ρ_{PAG} is the number of PAG molecules/volume, $\rho_D\left(\vec{r},t\right)$ is the density of deprotection (normalized to range between 0 and 1) at position $\vec{r}$ at time t, α is the resist absorptivity, q is the photon-PAG interaction volume (~1 nm^3), $E\left(\vec{r}\right)$ is the exposure doese at position $\vec{r}$ in units of the number of incident photons/area, D_A, D_B and D_{AA} are the diffusion coefficients of the acid, base and AA molecules respectively and k_D, k_{AB} and k_{AA} are the reaction rate constants for deprotection, acid-base neutralization and acid amplification, respectively.

The aerial image intensity $E\left(\vec{r}\right)$ is calculated in the standard fashion. The image used here is for a 50/50 nm line/space pattern, 1 micron long in the direction of the lines/spaces and 500 nm wide. We simplify the numerics by assuming that the exposure intensity and the acid, base and AA densities are uniform through the resist thickness, i.e., in z, and integrate out the z dependence. This effectively reduces the problem to 2D. Note that assuming that ρ_D, ρ_A, ρ_B and ρ_{AA} are independent of z and replacing each with itself multiplied by the resist

thickness h so that the new density values are in terms of the number of molecules/area requires dividing the 3D values of k_D, k_{AB}, and k_{AA} by h. This rescaling of the rate constants is the only vestige of the full 3D nature of the process that remains in our current simulation approach. Given a resist absorptivity α, photon-PAG interaction volume q and exposure dose $E(\vec{r})$ the initial acid distribution $\rho_A(\vec{r}, 0)$ is computed from Eq 1. We assume that the initial base and AA loadings $\rho_B(\vec{r}, 0)$ and $\rho_{AA}(\vec{r}, 0)$ are uniform throughout the resist and that $\rho_D(\vec{r}, 0) = 0$, i.e., the resist is protected. Full deprotection corresponds to $\rho_D = 1$.

There are many sources of stochastic behavior in the exposure and development processes. The primary one is wave function collapse.[23] When a photon is absorbed by the resist all of its energy goes into one molecule or atom of the resist. Hence, the smooth continuous aerial image is captured by the resist as a distribution of atoms or molecules at positions where the photons are absorbed. This is illustrated in Figure 1 for a sinusoidal image and is generally referred to as photon shot noise. There are also stochastic effects in the chemistry of the PEB and in the development step as well For DUV, i.e., 193 nm and 248 nm wavelengths, resists these effects are generally much smaller than those caused by wave function collapse.[15] At EUV, i.e, at around a wavelength of 13.5 nm, there is another source of stochastic effects during exposure which may not be negligable. At DUV wavelengths, in a chemically amplified resist the acids which deprotect the resist during the PEB are released directly by photon absorption by a PAG molecule. The photons that are absorbed by other molecules are similar to those that pass through the resist in that they cause no relevant chemical changes in the resist. Their absorption does decrease the remaining numbers of photons which does affect the final acid distribution but only indirectly. EUV photons have an energy of about 92 eV, as opposed to DUV photons which have energies on the around 5 eV. Hence the aborption of an EUV photon by any molecule or atom in the resist generally produces a photoelectron. This photoelectron can have an energy close to the EUV photon energy and as it travels through the resist can generate secondary electrons and when any of these electrons, primary or secondary, interacts with a PAG molecule they can cause it to release an acid. The process of secondary electron generation is certainly stochastic[16,17,18] and is often referred to as acid shot noise. It also adds to the net effective blur of the resist.[24,25] In addition to exposure statistics the initial distribution of PAG, base and AA molecules in the resist is also statistical. In our model these stochastic effects are included by replacing the nominal values of $E(\vec{r}), \rho_{PAG}, \rho_B(\vec{r}, 0)$ and $\rho_{AA}(\vec{r}, 0)$ in each 1 nm^2 area element by values chosen from a Poisson distribution

$$p(n|N) = \frac{N^n}{n!} e^{-N}$$

with mean value N equal to the given nominal value. Here $p(n|N)$ indicates the probability of getting n when the average value is N.After applying these statistics to the initial distributions PAG, acid, base and AA, the acid and base are assumed to completely neutralize one another before the start of the PEB.
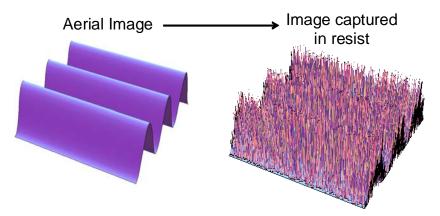

Figure 1: Illustration of the effect of wave function collapse, i.e., exposure statistics. On the left is a 50 nm period sinusoidal aerial image intensity, plotted, as usual, as a smooth continuous surface. On the right is the result of exposing that aerial image in resist. The Poisson statistics (discussed in the text) used to generate the plot on the right assumed a pixel size of 1 nm^2 and the exposure dose corresponded to 5 mJ/cm^2.

Individually the terms in the equations above describing just diffusion, acid-base neutraliztion, acid-AA amplification and deprotection are analytically solvable. Thus we can numerically solve the full set of equations by evaluating the analytical solution of only one of these processes during each time step, Δt.[20] That is, in the first time step solve analytically for just the diffusion of each species (acid, base and AA) in that time step, in the second time step solve analytically for just acid-base neutralization in that time step, in the third time step solve analytically for just acid-AA amplification in that time step and in the fourth time step solve analytically for the net level of deprotection given the net amount of acid. Each of these steps can then be repeated until the total PEB time is reached. The value of Δt used here was chosen small enough so that the end result of the simulations was relatively insensitive to the exact value of Δt. We found that a time step less than around 0.25 seconds was sufficiently small.

3   Results

Given the number of parameters in the model (3 diffusion constants, 3 rate constants and 4 initial density values, acid, base, PAG and AA) it is difficult to easily express the full range of dependencies especially when stochastic effects are included and doing this would require a much longer document than can be presented here. Instead, in order to get an idea of the range of dependencies we will simply show some sample results. Figure 2 illustrates the effect of "turning on" various statistics and Figure 3 is an example of the types of results available from the model.
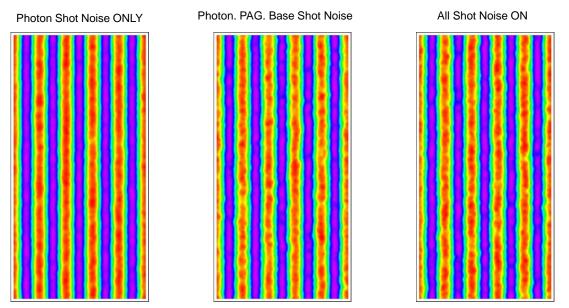

Figure 2: Examples of the effect of various statistics on the deprotection density which is normalized to range from 0 to 1.

ρ_{PAG}	0.2	0.2	0.2	0.2	0.2	0.2	0.2	0.2	0.2
$\rho_B(\vec{r},0)$	0.01	0.01	0.01	0.01	0.01	0.03	0.03	0.03	0.03
$\rho_{AA}(\vec{r},0)$	0.01	0.1	0.01	0.2	0.2	0.2	0.2	0.2	0.2
D_A	1.0	1.0	1.0	1.0	1.0	1.0	2.0	2.0	2.0
D_B	1.0	1.0	1.0	1.0	1.0	1.0	2.0	2.0	2.0
D_{AA}	1.0	1.0	1.0	1.0	1.0	1.0	2.0	1.0	3.0
k_{AB}	50.0	50.0	50.0	50.0	50.0	50.0	50.0	50.0	50.0
k_{AA}	0.01	0.01	0.1	0.1	0.4	0.4	0.4	0.4	0.4
E_{size}	13.0	13.0	13.0	7.0	2.0	8.0	7.2	6.8	11.3
CD	49.45	48.90	48.86	50.16	50.20	48.12	50.84	49.69	50.91
LER	1.74	1.63	1.61	2.27	6.96	2.87	5.63	7.00	2.07

Figure 3: The table shows example results with values in the table corresponding to 3D. The densities $\rho_{PAG}, \rho_B, \rho_{AA}$ are in units of nm^{-3}, the diffusion constants D_A, D_B, D_{AA} are in units of nm^2/s, the rate constants k_{AB} and k_{AA} are in units of nm^3/s, the sizing dose, E_{size} is in units of mJ/cm^2 and the mean linewidth (CD) and LER are in units of nm. The dose was chosen in each case to keep the CD to within about ± 1 nm of the nominal 50 nm linewidth when thresholding the deprotection level at 0.7. All values, except for CD and LER, are input values and hence have no uncertainty. The statistics obviously causes separate runs with the same input values to yield slightly different CD and LER values. Both the CD and LER obtained from multiple runs at fixed input values varied within a range of about ± 0.5 nm (1σ) which can therefore be taken as an indication of their uncertainty. As discussed in the text the density values, ρ, are multiplied by h, the resist thickness, whereas the rate constants k are divided by h in order to scale their 3D values to 2D. Here h was taken to be 50 nm.

The numbers in the table in Figure 3 tell only part of the story. Figures 4 and 5 show the average along the lines (Figure 2) of the initial and final acid, base and AA densities (in 2D units of nm^{-2}) and the net acid density. The LER PSD in Figure 4 has the shape and predicted slope of -3 on the log-log scale[15] as indicated by the straight line. This is not the case with the PSD in Figure 5. More work is required to understand the origin of this difference. Note the difference in AA and net acid densities.
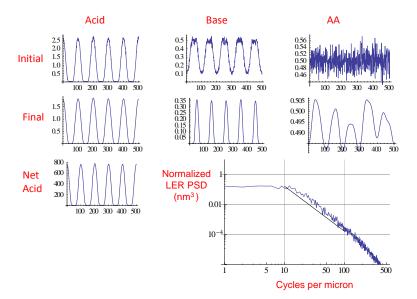
Figure 4: Initial and final acid, base, AA and net acid densities averaged along the length of the lines (see Figure 2) corresponding to the values in the first column of Figure 3. Density units are nm^{-2} corresponding to 2D values and the horizontal scale is nm. Note the difference in AA and net acid level between this result and that in Figure 5. The straight line in the LER Power Spectral Density (PSD) plot has a slope of -3 on the log-log scale. This is the slope predicted for the PSD.[15] The PSD in this case has the expected shape.
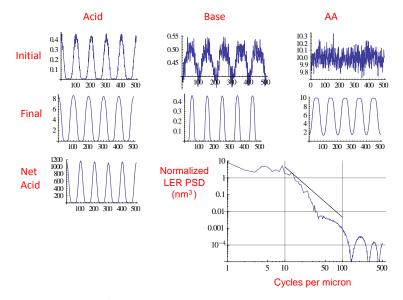

Figure 5: Initial and final acid, base, AA and net acid densities averaged along the length of the lines (see Figure 2) corresponding to the values in the sixth column of Figure 3. Density units are nm^{-2} corresponding to 2D values and the horizontal scale is nm. Note the difference in AA and net acid level between this result and that in Figure 4. The straight line in the LER Power Spectral Density (PSD) plot has a slope of -3 on the log-log scale. This is the slope predicted for the PSD.[15] The PSD in this case has does not have the expected shape.

When there is no AA present the standard relationship between LER and dose-to-size is LER $\sim 1/\sqrt{E_{size}}$.[15] Plotting the values of E_{size} and LER shown in the table in Figure 3 yields the plot in Figure 6. The solid cuve is $1/\sqrt{E_{size}}$ normalized to intersect the LER data at $E_{size} = 13$ mJ/cm^2 and corresponding to the first column in the Table in Figure 3 which contains very little AA and weak acid-AA coupling. The vertical bars indicate the estimated $\sim \pm 0.5$ nm (1σ) uncertainty in the computed LER values as determined by multiple runs with the same mean input values.

Figure 7 shows values of line width roughness (LWR) as a function of Dose $= E_{size}$ computed over a much larger range of parameter variation than is shown in Figure 6. (Note: When the roughness on each edge of each line is uncorrelated then the overall LWR value is, to a good approximation, $\sqrt{2}$ times the mean LER value of the edges.) The red lines indicate the average and $\sim \pm 0.8$ nm (1σ) statistical variation in LWR with no AA present but with the base loading changed in order to vary E_{size}. In contrast to experimental data, which appears to show an improvement in the RLS tradeoff using AAs,[6] the modeling results, at least so far, show no great difference between AA and non-AA behavior. This is probably because the experimental improvement appeared to come from reduced top loss,[6] something which is not currently captured in the 2D implementation of the model used here.
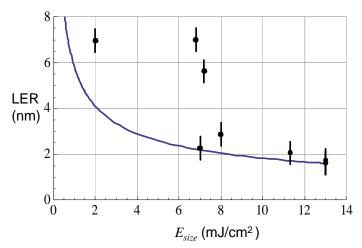

Figure 6: Plot of LER and E_{size} from the table in Figure 3. The solid cuve is $1/\sqrt{E_{size}}$ normalized to intersect the LER data points at $E_{size} = 13$ mJ/cm^2. The vertical bars indicate the estimated ± 0.8 nm (1σ) uncertainty in the the computed LER values. In contrast to published experimental data[6] it appears that acid amplifiers are not helping with the RLS tradeoff.[2] This is probably because the model at this stage does not include the relevant parameters.
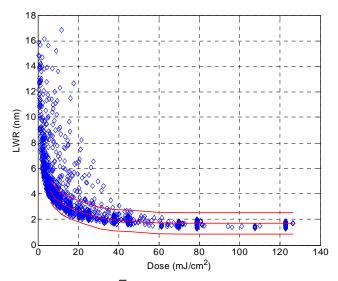
Figure 7: Line Width Roughness (LWR $\sim \sqrt{2}\times$ LER) versus Dose $= E_{size}$ for a wide range of input values. Base loading varied from 0.01 nm^{-3} to 0.1 nm^{-3}, AA loading varied from 0.1 nm^{-3} to 2.0 nm^{-3}, k_{AA} varied from 0.001 nm^3/s to 4.0 nm^3/s at PAG loading of 0.2 nm^{-3}, $k_D = 1.5$ nm^3/s, $k_{AB} = 1.5$ nm^3/s, $D_A = D_B = D_{AA} = 1.1$ nm^2/s. The red lines indicate the mean and $\sim \pm 0.8$ nm (1σ) range of variation of LWR for runs done with no AA but with varying base loadings.

4   Conclusions

We have presented a fully stochastic model of resist exposure and deprotection during PEB. The initial objective of this work was to evaluate the capability of acid amplifiers (AAs) to make significant in-roads towards improving in the RLS trade-off.[2] What the model shows so far is that chemically amplified photoresists are still governed by the basic principles of the RLS trade-off with or without AAs. What the model does not address is the comparison between resist formulations in which combinations of polymer, PAG, base and AA may provide the best RLS performance, within the limitations to the RLS trade-off, such has been shown experimentally.[6] The improvement seen in the experimental data seems to comes from the AA inhibiting the top loss. This is something that cannot be captured in the current 2D implementation of the model. The other possible interpretation of the experimental data can be gleaned from Figure 7. Note that although there is a spread of LWR values at each dose there appears to be a mimimum possible "hard stop" value of LWR at each dose. It may be that the experimental improvement seen using AA involves migrating a given resist from above the "hard stop" down to it. In order to do a more direct comparison with experimental data we do need to expand the model to 3D.

5   REFERENCES

[1] M. D. Shumway, et. al., J. Vac. Sci. Tech. **B23**, 2844 (2005).

[2] G. M. Gallatin, et. al., Proc. SPIE **6921**, 69211E/1, (2008).

[3] R. L. Brainard, et. al., Proc. SPIE **5374**, 74 (2004).

[4] K. Ichimura, Chemical Record **2**, 46 (2002).

[5] C. J. Gerdts, et. al., J. Am. Chem. Soc.**126**, 6327 (2004).

[6] S. Kruger, et. al., J. Photopol. Sci. Tech. **24**, 143 (2011).

[7] S-W. Park, et. al., Macromolecular Rapid Communications **21**,1050 (2000).

[8] S. Noguchi, et.al., J. Photopol. Sci. and Tech. **10**, 315 (1997).

[9] O. T. Naito, et. al., J. Photopol. Sci. and Tech. **12**, 509 (1999).

[10] S-W. Park, et. al., J. Photopol. Sci. and Tech. **12,** 293 (1999).

[11] K. Kudo, et. al., Chemistry of Materials **11**, 2119 (1999).

[12] H. Ito, and K. Ichimura, Macromolecular Chemistry and Physics **201**,132 (2000).

[13] K. Arimitsu, et. al., J. Am. Chem. Soc. **120**, 37 (1998).

[14] S. Lee, et.al., J. Photopol. Sci. and Tech. **13,** 215 (2000).

[15] G. M. Gallatin, Proc. SPIE **5754**, 38 (2005).

[16] D. Drygiannakis, et. al., Proc. SPIE **6519**, 65193T (2007).

[17] J. Biafore, et. al., Proc. SPIE **7636**, 76360R-1 (2010).

[18] C. Mack, et. al., Proc SPIE **7969**, 7969-43, to appear, (2011).

[19] G. M. Gallatin and P. P. Naulleau, Proc SPIE **7969**, 796903 (2011).

[20] H. Fukuda, et. al., Proc. SPIE **4346**, 319 (2001).

[21] P. P. Naulleau, G. M. Gallatin, J. Vac. Sci. Technol. **B 28**, 1259 (2010).

[22] C. Mack, *Fundamental Principles of Optical Lithography* (Wiley, West Sussex, England, 2007, Chapter 7, page 257).

[23] R. P. Feynman, R. Leighton and M. Sands, *The Feynman Lectures on Physics* (Addison-Wesley 1965, Vol 3. Chapter 1).

[24] C. N. Anderson, et. al., J. Vac. Sci. Technol. **B 26**, 2295 (2008).

[25] G. M. Gallatin, et. al., Proc. SPIE **6519**, 651911 (2007).